HHS Public Access

Author manuscript

Immunobiology. Author manuscript; available in PMC 2023 January 17.

Published in final edited form as:

Immunobiology. 2020 September ; 225(5): 152003. doi:10.1016/j.imbio.2020.152003.

Absence of complement factor H reduces physical performance in C57BL6 mice

Kenneth L. Seldeen[b], **Ramkumar Thiyagarajan**[b], **Yonas Redae**[a], **Alexander Jacob**[a], **Bruce R. Troen**[b,c], **Richard J. Quigg**[a], **Jessy J. Alexander**[a,*]

[a]Department of Medicine, Division of Nephrology, Jacobs School of Medicine and Biomedical Sciences, University at Buffalo, Buffalo, NY, USA

[b]Geriatrics and Palliative Medicine, Jacobs School of Medicine and Biomedical Sciences, University at Buffalo, Buffalo, NY, USA

[c]Research Service, Veterans Affairs Western New York Healthcare System, Buffalo, NY, USA

Abstract

Complement (C) system is a double edge sword acting as the first line of defense on the one hand and causing aggravation of disease on the other. C activation when unregulated affects different organs including muscle regeneration. However, the effect of factor H (FH), a critical regulator of the alternative C pathway in muscle remains to be studied. FH deficiency results in excessive C activation and generates proinflammatory fragments C5a and C3a as byproducts. C3a and C5a signal through their respective receptors, C5aR and C3aR. In this study, we investigated the role of FH and downstream C5a/C5aR signaling in muscle architecture and function. Using the FH knockout (fh−/−) and fh−/−/C5aR−/double knockout mice we explored the role of C, specifically the alternative C pathway in muscle dysfunction. Substantial C3 and C9 deposits occur along the walls of the fh−/− muscle fibers indicative of unrestricted C activation. Physical performance assessments of the fh−/− mice show reduced grip endurance (76 %), grip strength (14 %) and rotarod balance (36 %) compared to controls. Histological analysis revealed a shift in muscle fiber populations indicated by an increase in glycolytic MHC IIB fibers and reduction in oxidative MHC IIA fibers. Consistent with this finding, mitochondrial DNA (mtDNA) and citrate synthase (CS) expression were both reduced indicating possible reduction in mitochondrial biomass. In addition, our results showed a significant increase in TGFβ expression and altered TGFβ localization in this setting. The architecture of cytoskeletal proteins actin and vimentin in the fh−/− muscle was changed that could lead to contractile weakness and loss of skeletal muscle elasticity. The muscle pathology in fh−/− mice was reduced in fh−/−/C5aR−/− double knockout

*Corresponding author. jessyale@buffalo.edu (J.J. Alexander).

Author contributions

KLS, YR, RT, AJ. conducted experiments and analyzed data. JJA designed, participated in conduct of experiments, analyzed the data and wrote the manuscript. BRT and RJQ participated in designing the experiments and edited the manuscript.

Ethics approval

All studies and experimental protocols were approved by and in compliance with guidelines of the University at Buffalo Animal Care and Use Committees.

Declaration of Competing Interest

The authors report no declarations of interest.

(DKO) mice, highlighting partial C5aR dependence. Our results for the first time demonstrate an important role of FH in physical performance and skeletal muscle health.

Keywords

Complement; Factor H; Muscle; Inflammation; Extracellular matrix

1. Introduction

The complement (C) system is an important component of muscle inflammation that occur in settings such as in autoimmune disease, and modified muscle use (Sewry et al., 1987; Spuler and Engel, 1998; Walport, 2001a, b; Zipfel and Skerka, 2009). C proteins (Wang et al., 2017) participate in functions such as inhibition and restoration of muscle regeneration (Naito et al., 2012; Zhang et al., 2017) and in recruitment of macrophages (Wang et al., 2017). However, the role of complement factor H (FH) in muscle health and disease remains unknown. FH (FH) is an important C regulator generated mostly by the liver (Pangburn, 1988) and also by other organs, including muscle (Alexander and Quigg, 2007; Ferreira et al., 2010). (Legoedec et al., 1995). FH is traditionally involved in innate host defense, but also participates in noncanonical roles such as immune-evasion, regulation of B-cell differentiation and platelet activation (Alexander and Quigg, 2007; Ferreira et al., 2010). In addition to FH, the role of other complement proteins such as C3, C3a and C5a in muscle health is just beginning to emerge (Puri and Quigg, 2007; Sorgenfrei et al., 1982). (Behan and Behan, 1977). C causes lysis of muscle membranes in myasthenia gravis (Ashizawa and Appel, 1985) and C3 and C9 deposition in necrotic fibers (Cornelio and Dones, 1984; Morgan et al., 1984). C5b-9 can lead to a loss in membrane integrity and necrosis of the targeted cells (Mathey et al., 1994; Schafer et al., 1986). However, the exact underlying mechanism/s by which C activation causes alteration in muscle needs to be explored.

Muscle function is closely related to the fiber population and quantity of connective tissues between fibers (Richmonds and Kaminski, 2001). Skeletal muscle is composed of a mosaic of muscle fiber types (type I, type IIA, type IIB, and type IIX), which have different amounts of myosin heavy chain (MHC) proteins, mitochondria, and capillary density, and different susceptibility to loss of strength and fatigue. Based on the MHC isoforms skeletal muscle is characterized as both oxidative slow twitch fibers with a higher mitochondrial density (type I and type IIA) (Buckingham et al., 1986; Schiaffino et al., 1989; Staron et al., 1990) and glycolytic fast twitch fibers more reliant on glycolysis to metabolize glucose (types IIb) that differentially impact muscle metabolism (Clarke et al., 1975; Gulick et al., 1997; Moncman et al., 1993). The maximum velocity of contraction (Vmax) for fibers composed of a single MHC increases in the order type I, IIA, IIX, IIB (Bottinelli et al., 1991; Galler, 1994). Intermediate hybrid fibers, containing type I and IIA, can be observed in normal muscles. Muscle is a dynamic organ in which fiber type shifts take place, either in response to exercise or electrical stimulation or during muscle wasting associated with atrophying conditions. The optimal functioning of the different fibers are based on the energy demands being met, which is maintained by fine tuning of the mitochondrial density and function (Zong et al., 2002). ATP generation in muscle occurs by both glycolysis

and mitochondrial function (Rangaraju et al., 2014). Since both fiber composition and metabolic properties affect function, it is interesting to know the extent to which they co-vary. Muscle cytoarchitecture is another important aspect underlying muscle integrity and function. Cellular cytoskeleton network can induce protein conformational change (Sawada et al., 2006) leading to disruption of intermediate filaments resulting in a number of diseases (Traub and Shoeman, 1994). The actin cytoskeleton undergoes dynamic assembly and disassembly during cell migration and adhesion (Tang and Gerlach, 2017) and therefore is regulated by a variety of actin-associated protein and signaling pathways, including the vimentin network and by members of the TGFβ family (Jiu et al., 2017).

In brief, for the first time our study presents evidence that CFH deficiency in mice results in reduced muscle strength, altered muscle fiber composition and a concomitant reduction in mitochondrial DNA and citrate synthase activity compared to the wildtype animals. Our results demonstrate that C activation plays a critical role in muscle pathogenesis in an inflammatory setting and reveal its potential as a therapeutic target.

2. Material and methods

2.1. Mice

Complement FH knockout (fh−/−) mice obtained from Drs Matthew Pickering and Marina Botto (Imperial College of London) (Pickering et al., 2002) were backcrossed onto C57BL/6 mice for 20 generations. $C5aR^{-/-}$ mice were provided by Drs Allison Humbles and Craig Gerard (Harvard Medical School), and backcrossed at least 12 generations onto normal C57BL/6 mice (Jackson Laboratories, Bar Harbor, ME) (Hopken et al., 1997). To generate fh−/−/C5aR−/− double knockout (DKO) the fh−/− male were crossed with C5aR−/− female. The heterozygous progeny were bred among themselves to generate progeny that were DKOs. Genotyping for FH and C5aR alleles was performed using PCR-based approaches. Age matched wild type (WT) C57BL/6 mice were maintained in the same facility as controls. Male mice aged 16 and 24 weeks, n = 8 were used for the experiments. Mice were housed 2–3 per cage and provided *ad libitum* access to both food and water, and facility lighting was on a standard 12 h light/12 h dark schedule. Body weight was determined using a digital scale (model CS200; Ohaus, Pine Brook, NJ).

2.1.1. Body composition—Whole body lean and fat mass were determined using quantitative magnetic resonance with a Bruker LF65 (Bruker, Germany), data from scans of mice were compared to a standard curve generated from known masses of lean chicken breast and lard. Determinations of body composition were based on the average of 2 scans per mouse.

2.1.2. Functional assessments of physical performance—Physical performance assessments were performed as described in (Seldeen et al.). Investigators were blinded to the identity of the mice and all assessments were performed by the same experimenter and at a similar time of day. Performance assessments include:

2.1.3. Grip strength—Grip strength assessment was performed using a digital mouse grip strength meter (Columbus Instruments, Columbus OH). Mice were scored as the best

3 of 5 trials to avoid habituation. The mouse was allowed to grip a wire mesh grid with its front paws and then was gently pulled away by its tail until it released the grid. The maximum resistance force (mN) generated when the animal is being pulled away from the instrument and it loses its grip, was recorded by a force transducer attached to the grid, and mice were given 10 s rest between trials. Increase in grip strength is considered evidence of increased muscle strength and vice versa, decrease in grip strength is considered a sign of muscle weakness and fatigue. Multiple trials were done to generate reliable data and obtain statistics while the trails were limited to 3 to avoid habituation.

2.1.4. Grip endurance—Grip endurance test also known as Kondziella's inverted screen test is used to test the overall strength of all four limbs. A grid apparatus was designed to allow mice to grab the 30cm × 30cm - 1.27 cm^2 wire mesh and then the grid was inverted 180 degrees onto a 45 cm tall box to test mouse grip endurance. The time before the mice dropped off of the grid on to a soft pad below was recorded for each assessment with a maximum time of 300 s. Mice were scored as the average of the best two of three trials.

2.1.5. Rotarod performance—One month prior to assessment the mice are acclimated to the device by providing three trials whereby the rotarod device (Med Associates Inc., Fairfax, VT) accelerates from 2 to 20 revolutions per minute (RPM) over 5 min. For assessment, the mice are scored on the best 2 of 3 trials as the device accelerates from 4 to 40 RPM over 5 min.

2.1.6. Treadmill assessment—One month prior to the assessment, the mice are acclimated to the treadmill device (Columbus instruments) whereby the mice are given three trials where the treadmill increases from 5 to 10 m/min over 5 min. Two weeks prior to the assessment, the mice are given a single trial where the device increases from 5 to 20 m/min over 30 min. For assessment, mice are given a single trial with the treadmill belt inclined at 5° where the mouse is scored for total time on belt before exhaustion as the belt speed increases from 5 to 35 m/min over 60 min. Exhaustion is defined as the mouse visiting the shock grid 10 times or receiving 20 total shocks (0.2 mA).

2.2. Histological assessments

2.2.1. NADH staining of muscle—Gastrocnemius muscle was harvested and vertically mounted on cork plates using OCT compound and liquid nitrogen. Cryosections of 10 μm thickness were collected and were subjected to NADH-tetrazolium Reductase (NADH-TR) staining (Zong et al., 2002). Sections were incubated in 0.2 M Tris, pH 7.4, containing 1.5 mM NADH and 1.5 mM nitrotetrazolium blue for 30 min at 37 °C. Sections were placed in different concentrations of acetone solutions (30, 60, 90, 60, and 30 %) for 2 min each and mounted with Aquamount (Lerner Labs, Pittsburgh, PA). Type I fibers are primarily oxidative fibers and stain darkly with this stain. Type IIA fibers are a mix of both oxidative and glycolytic fibers and Type IIB fibers are primarily glycolytic and thus stain lightly with this stain (Seldeen et al., 2017). All samples were prepared and processed equally at the same time, and all images were taken at the same exposure level. The fibers in 2 entire stained sections from a gastrocnemius mouse muscle (n = 8/group) was analyzed. Each

gastrocnemius muscle stained by NADH-TR was photographed at 40× magnification for assessment of fiber-type composition.

2.2.2. Immunostaining—The gastrocnemius (GCN) muscles were isolated from all mice and rapidly frozen in precooled isopentane. A small amount of fresh embedding medium (Tissue-Tek O.C.T. (optimal cutting temperautre) compound (Sakura Finetek, Torrance, CA, USA)) was placed on a chuck (cork) and the base of the muscle was immersed in it maintaining the cross-sectional orientation. Two 8-μm thick sections of the muscle specimen collected on Superfrost-Plus glass slides were fixed by the addition of 4% paraformaldehyde in ice-cold PBS for 10 min. To immunostain cell-surface antigens, cells were blocked for 1 h with 1% BSA in PBS and then probed with the relevant primary antibodies.

All antibody cocktails are prepared in block solution (10 % goat serum in PBS). Antibodies SC-71 and BF-F3 were obtained from Developmental Studies Hybridoma Bank (University of Iowa), whereas secondary antibodies were purchased from Invitrogen (Bloemberg and Quadrilatero, 2012). A polyclonal C9 Ab (raised in rabbit) reactive with rat/mouse (provided by Dr. B. P. Morgan, University of Wales College of Medicine, Cardiff, U.K.) was used to stain for mouse MAC. FITC-conjugated anti-rabbit IgG (Sigma-Aldrich) was used as the secondary Ab. Control stains were performed with normal rabbit serum at concentration similar to that of primary Ab. Additional controls consisted of staining by omission of the secondary Ab. Immunofluorescent probes were illuminated by epifluorescence and were visualized through red (filter set 45 HQ Texas red shift free), green (filter set 44 FITC special shift free) and blue (filter set 49 DAPI shift free) band-pass filters (Carl Zeiss, Cambridge, UK) on an AxioPlan microscope (Carl Zeiss; 10×, 20×, 40× objectives with 0.25, 0.75, 0.95 numerical apertures, respectively). To ensure strict comparability, sections were photographed at identical exposures and in the same microscopy session.

2.2.3. Gene expression and mitochondrial DNA abundance—RNA was extracted from gastrocnemius (GCN) muscle of the two groups of mice using TRIzol (Invitrogen, Carlsbad, CA) as described previously (Alexander et al., 2005). The concentration of mRNA was measured by Nanodrop ND-2000C (Thermo Scientific). cDNA was synthesized from 2 μg mRNAs using the QuantiTect RT kit (Qiagen). The mRNA levels of genes were analyzed by qRT-PCR, which were performed with 2 × SYBR master mix (Takara, Otsu, Shiga), using BIO-RAD CFX CONNECT system (Bio-Rad). qPCR primers are given in Table 1. Threshold values using 18S measured contemporaneously from the same samples served as control. (Ct; gene relative expression = $2^{[Ct\ (18S) - Ct\ (target\ gene)]}$. Mitochondrial DNA abundance (mtDNA) was quantified by qRT-PCR. In short, DNA was extracted using the standard phenol extraction method, and the resulting genomic DNA (gDNA) was used for qPCR using the primers in Table 2. The ratio of mt:nuclear DNA reflects the tissue concentration of mitochondria per cell. Quantification was performed in a total reaction volume of 25 μl containing: 2X SYBR Green (12.5 μl), each primer (1.25 μl), sample DNA (1 μl), and water (9 μl). Annealing temperature was at 49 °C. Samples were assayed in triplicate. Data analysis was based on measurement of the cycle threshold (C_T), and the difference in C_T values was used as the measure of relative abundance: C_T(ND1)

− C_T(mt DNA) or ΔC_T, a quantitative measure of the mitochondrial genome. Results were expressed as the copy number of mtDNA per cell, provided by $2 \times 2^{-\Delta}C^T$.

2.3. Biochemical assessments

2.3.1. C3 assessment—C3 in the plasma was determined using the mouse C3 ELISA kit from Molecular Innovations (cat # MC3KT) according to the manufacturer's instructions. All reagents and standards are provided with the kit. The ELISA plate was coated with mouse C3 capture antibody. Plasma and serum samples were diluted 1:100,000 to 1:1,000,000. Mouse C3 bound to the capture antibody coated on the microtiter plate. After 3X washes, HRP labeled anti-mouse C3 primary antibody is incubated with the captured protein. Following an additional washing step, TMB substrate is used for color development at 450 nm. Color development is proportional to the concentration of C3 in the samples. A standard calibration curve is prepared using dilutions of purified C3 and is measured along with the test samples. All reagents and standards are provided in these ELISA kits. In a similar fashion, plasma C5a content was determined using a sandwich ELISA (DuoSet ELISA, cat DY2150) from R&D Systems (Minneapolis, MN, USA).

2.3.2. Calcium assay—Calcium levels in serum was assessed using the arsenazo reagent. Calcium ions (Ca2+) react with Arsenazo III (2,2′-[1,8-Dihydroxy-3,6-disulphonaphthylene-2,7-bisazo]- bis benzene arsonic acid) to form an intense purple colored complex.2,3 The absorbance of the Ca-Arsenazo III complex is measured bichromatically at 660/700 nm. The resulting increase in absorbance of the reaction mixture measured using Synchron CX System is directly proportional to the calcium concentration in the sample.

2.3.3. Measurement of citrate synthase activity—Citrate synthase (CS) activity is considered a representative enzyme for mitochondrial respiratory capacity (Powers et al., 1992). CS was determined in GCN muscle extracts spectrophotometrically (Ceddia et al., 2000). GCN muscles (20 mg) were homogenized on ice in 0.1 M Tris buffer containing 0.1 % Triton X-100, pH 8.35. The assay system contained in a total volume of 200 μL:100 mM Tris buffer (pH 8.35), 5 mM 5,5- dithiobis(2-nitrobenzoate) (DTNB), 22.5 mM acetyl-CoA, 25 mM oxaloacetate (OAA), and 4 μL of homogenate of muscle. The reaction of acetyl-CoA with OAA was initiated and linked to the release of free CoA-SH to a colorimetric reagent, DTNB. The rate change in color was monitored at wavelength of 405 nm by using a Dynex MRX plate reader (Revelation, Dynatech Laboratories). All measurements were performed in duplicate. The solubilized protein extracts of the homogenates were quantified in duplicate by using bicinchoninic acid reagents (Pierce, Rockford, IL) and bovine serum albumin standards. The CS activity was then normalized to the total protein content and was reported in as nanomoles per milligram protein per minute.

2.3.4. Statistical analysis—Results were analyzed using the Minitab software and are expressed as Mean ± S.D, n = 8/group. Statistical comparisons between two groups were evaluated by unpaired Student's t-test, two-tailed or two way repeated measures ANOVA followed by Bonferroni post-test. Probability (P) value <0.05 was considered statistically significant.

3. Results

3.1. Preliminary workup

Body weight and fat % were assessed in16 week male mice of both wt and fh−/− groups. Although the increase in body weight and fat% in fh−/− mice compared to controls did not reach statistical significance, 6 out of 8 fh−/− mice showed an increase in body wt compared to controls indicating that the absence of FH contributed to the increase in body wt. Since calcium ions are important in the maintenance of normal muscle contractility, calcium levels in serum was assessed. Circulating calcium levels (nmol/L) remained unchanged (Table 3).

3.2. Absence of FH increases expression of complement proteins

To determine the expression of complement proteins in muscle in the absence of FH, gastrocnemius muscle was subjected to real-time PCR with gene specific primers (Fig. 1A). The expression of FH, the core complement protein C3 and the downstream anaphylatoxin receptors, C3aR and C5aR were assessed. As expected FH was not expressed in fh−/− muscle. However, the expression of C3, C3aR and C5aR1 were significantly increased in fh−/− muscle compared to controls, n = 8 mice/group.

Ablation of FH results in unregulated activation of the alternate pathway and increased consumption of circulating C3 (Pickering et al., 2002). Indeed, the plasma levels of C3 decreased to one fifth the controls in fh−/− mice while there was a threefold increase in plasma C5a compared to controls (Fig. 1B). Immunofluorescence staining of muscle sections for FH (green) and C5aR (red) indicated that these proteins were expressed in the muscle as shown earlier (Kouser et al., 2013) and were membrane bound (Fig. 1C)

3.3. Absence of CFH increases complement activation in muscle

To determine whether C3 and C9 deposits occurred in muscle of fh−/− mice similar to that observed in kidneys (Pickering et al., 2002), we stained muscle sections (representative sections are given) of wt and fh−/− mice with antibody against C3 and C9 (membrane attack complex (MAC) (Fig. 2). Immunofluorescence analysis of GCN muscles showed C3 deposits (upper panel) was limited in the *wt* muscle (Fig. 2A), while a more significant pattern of deposits were observed in $fh^{-/-}$ muscle (Fig. 2B). Similar to that observed in the kidney, C3 deposits in the fh−/− muscle occurred along the cell walls. C9 deposits that were nearly nonexistent in wt muscle (Fig. 2D) was evident in the fh−/ muscle (Fig. 2E). Both C3 (Fig. 2C) and C9 (Fig. 2F) expression remained unchanged in the absence of C5aR.

3.4. Ablation of CFH decreases oxidative capacity and increases glycolytic myofibers

To understand whether muscle fiber switching occurred in fh−/− mice, we next determined the fiber-type composition in GCN muscle using enzyme histochemistry for NADH-tetrazolium reductase (NADH-TR), a mitochondrial enzyme in complex I (Fig. 3). NADH-TR staining reveals ATPase activity which correlates with oxidative capacity of the muscle. The oxidative capacity of muscle fibers follows the pattern type I (dark), IIA, IIX, IIB (light) (Aigner et al., 1993; Hamalainen and Pette, 1993). This study focused mainly on the Type II fibers. Type IIA fibers were significantly reduced with a concomitant increase in IIB fibers (Fig. 3B) in fh−/− mice compared with those of WT mice (Fig. 3A). These results

were further substantiated by MHC fiber typing using immunofluorescence. In line with the NADH-TR staining, fiber type MHC IIA was decreased and MHC IIB was increased in fh−/− mice (Fig. 3F) compared to wt controls (Fig. 3E). The unstained areas are a mix of fiber type MHC I and fiber type IIX. Interestingly, there was a significant increase of MHC IIA fibers in the fh−/−C5aR−/− mice (Fig. 3G), while the MHC IIB fibers were reduced closer to normal.

3.5. Absence of CFH reduces mitochondrial DNA in muscle

Next we investigated the impact of FH on mitochondrial density in the gastrocnemius muscle. In line with changes in fiber type, we observed significantly lower mRNA expression of mitochondrial encoded genes *(COX, UCP and HK)* by qRT-PCR in gastrocnemius muscle (Fig. 4A). The reduction in mitochondrial gene expression was prevented in the fh−/−C5aR−/− double knockout mice. Since mtDNA may not always be a reliable predictor for mitochondrial abundance, we assessed citrate synthase, a mitochondrial matrix enzyme that is representative of the mitochondrial content and an indicator for aerobic capacity and mitochondrial abundance in tissues (Cayci et al., 2012). Reduction of citrate synthase activity further substantiated the reduction of mitochondrial content in gastrocnemius muscle (Fig. 4B).

Absence of CFH alters expression of TGFβ and intermediate filaments proteins, vimentin and actin in muscle

In the present study absence of FH expression resulted in reorganization of cytoskeletal proteins. Actin and the intermediate filament vimentin that had a defined localization along the periphery of the cell in WT mice (Fig. 5A & D) changed to a more disrupted and less defined localization within the cell in fh−/− mice (Fig. 5B & E). Although there was little change in the expression of the proteins it was more defined, localized closer to the periphery wall in the absence of C5a/C5aR signaling (Fig. 5C & F). Since TGF-β members are involved in organization of cytoskeletal architecture, we assessed transforming growth factor-β (TGF-β) in the muscle. (Fig. 6). TGF-β was expressed at the sarcoplasmic membrane in the WT controls (Fig. 6A). (➘) (Ahn et al., 2009). In the absence of FH, TGFβ occurred in the endomysium (▶) Fig. 6B). TGFβ expression was on the sarcoplasmic membrane similar to controls in the absence of C5a/C5aR signaling (Fig. 6C). These changes were also observed at the transcriptional level (Fig. 6D).

3.6. Absence of FH affects skeletal muscle performance

To test the role of FH in muscle performance, we performed four different tests. Interestingly, absence of FH in 16 week old mice caused significant reduction ($p < 0.05$) in motor coordination, muscle strength, and grip endurance. The alteration in muscle performance was revealed in the rotarod latency to fall (204 ± 31 s vs 128 ± 25 s), grip meter strength (93 ± 8 vs 80 ± 11) and grid hang latency to fall (61.3 ± 8.5 s vs 15 ± 7.8 s) (Fig. 7) tests, respectively. In addition, fh−/− mice demonstrate a trend for lower treadmill endurance (285 ± 63 m vs 236 ± 49 m, $p = 0.06$) results not shown. The decrease in muscle strength was significantly aggravated by age. At 24 weeks grid hang (7.3 ± 5.7), rotarod (115 ± 28) and grip meter tests (62 ± 10). Treadmill (214 ± 43) tests also revealed

reduced activity, compared to mice at 16 weeks. However, since these mice potentially develop kidney disease when they reach 24–32 weeks of age (Pickering et al., 2002), all other assessments were made in 16-week-old mice with these compounding factors absent.

4. Discussion

Our recent studies showed that FH altered bone health and architecture (Alexander et al., 2018). The most important and novel finding of this study is that in the absence of FH, C activation alters muscle architecture and fiber composition that leads to reduced muscle strength and function, which worsened with age. Our results show increased deposits of C3 and C9 in the muscle indicating that complement activation occurred through the alternative pathway resulting in the formation of C9 or membrane attack complex (MAC). Furthermore, the decreased abilities in noninvasive tests such as grip meter, grid hang indicate muscle weakness and increased fatigue, while the reduced time in the rotarod test indicates reduced motor coordination.

C activation in the absence of FH leads to the generation of proinflammatory anaphylatoxins C3a and C5a, which signal through their G-protein coupled receptors C3aR and C5aR respectively. Elegant studies by Zhang et al. (Zhang et al., 2017) recently showed that the C cascade has a key role in macrophage recruitment and subsequent muscle regeneration after injury and that it proceeded through C3a-C3aR signaling. Our studies give further insight and show that C activation *per se* in the absence of any compounding injury alters muscle strength and function, such as the marked decline in muscle mass and function in skeletal muscle with age. In addition, our results show that the effects of FH depletion is partially dependent on C5a/C5aR signaling.

Muscles occupy 40 % of body mass and the muscles work in coordination with other muscles. Muscle has the ability to remodel and transform in response to the environmental demands (Booth et al., 2002; Schiaffino and Reggiani, 2011). Type I “slow twitch” fibers use oxidative phosphorylation for energy production and support sustained aerobic activity with increased contraction endurance and lesser strength potential. On the other hand, type IIB “fast twitch” fibers rely heavily on anaerobic glycolysis for energy production and have considerable strength and contraction speed, but only for short anaerobic bursts of activity before the muscles fatigue. An example is in endurance exercise training that induces a myofiber shift from a fast twitch type II fibers to slow twitch type 1 fibers (Booth et al., 2002). Our studies show that in the setting of C activation the reverse happens and the muscle fibers switch from slow to fast fiber types. The predominance of type II fibers, especially subtype B, indicates that the muscle presents a weak oxidative metabolism and is prone to fatigue during prolonged work (Bonington et al., 1987; Bredman et al., 1992). Muscle requires energy for optimum functioning. Our studies showed that along with the fiber switch, the muscle metabolic profile is altered, along with decrease in mitochondrial content. This is consistent with the previously established distribution of mitochondrial content across fiber types in mouse muscles (Shortreed et al., 2009). In addition this is also in line with increased endurance as measured by a treadmill endurance test. Since mitochondria are the main source of cellular energy and is critical in maintaining the functional and structural integrity of tissues such as muscle (Nair, 2005).

tissues with high-energy turnover such as muscle are particularly vulnerable to changes in energy metabolism caused by alteration in mitochondrial function thereby leading to tissue degeneration (Saraste, 1999).

Our studies show that TGFβ is upregulated in muscle in the absence of CFH with its localization moving from the sarcoplasmic membrane to the endomysium (Araujo et al., 2013). This is also in line with our observations of an altered mitochondrial profile with C activation since TGFβ is known to increase mitochondrial fragmentation (Krick et al., 2008) and alter mitochondrial metabolism (Pacher et al., 2008; Yoon et al., 2005). In addition, increases in TGFβ cause increases in extracellular matrix proteins, accompanied by incomplete tissue regeneration that can subsequently lead to fibrosis (Hinz, 2015). Mechanical properties of muscle is determined by cytoskeletal and intermediate filament network that are involved in migration, differentiation and signaling. Earlier studies demonstrate a central role for actin and vimentin in the cells mechanical properties (Charrier and Janmey, 2016; Eckes et al., 1998; Guo et al., 2013). TGFβ targets the cytoskeleton and intermediate filaments which provides a framework that integrates the components of the cytoskeleton and organizes the internal structure of the cell. The loss of actin and vimentin layer integrity in our study, along with all the other changes could lead to muscle weakness and loss of function observed in the fh−/− mice. The muscle changes that occur in the absence of FH are reduced in the absence of C5a/C5aR signaling indicating there are other factors that contribute to the pathology which could include C3a/C3aR signaling that was described recently. Future studies are required to further detail the signaling mechanisms and other underlying factors that are involved in causing these changes.

In conclusion, our study demonstrates for the first time an important role for FH in regulating muscle health and function. With a focus on the GCN muscle, the present study has found in the absence of FH, there is an alteration in skeletal muscle fiber content, change in mitochondrial function, increased TGFβ expression and changes in intermediate filaments that are partially dependent on C5a/C5aR signaling. These changes could have significant impact on the architectural arrangement of the muscle and remodeling of the extracellular matrix that could compromise muscle function and lead to muscle weakness. How the aforementioned outcomes are interlinked and whether the response to complement activation is similar in other muscles such as smooth muscles warrants further investigation. In addition, the fact that the absence of FH causes these changes underscores its importance as a potential therapeutic target in the setting of muscle inflammation.

Funding

This research is supported by NIH R01 Grant DK111222 to JJA, an endowment from Dr Arthur M. Morris to RJQ and the Veteran Affairs Rehabilitation Research and Development Grant RX001066 and the Indian Trail Foundation to BRT.

Abbreviations:

FH	complement factor H
TGFβ	transforming growth factor B

MHC	myosin heavy chain
GCN	gastrocnemius
NADH-TR	NADH-tetrazolium reductase
C5aR	C5a receptor

References

Ahn YO, Lee JC, Sung MW, Heo DS, 2009. Presence of membrane-bound TGF-beta1 and its regulation by IL-2-activated immune cell-derived IFN-gamma in head and neck squamous cell carcinoma cell lines. J. Immunol 182, 6114–6120. [PubMed: 19414763]

Aigner S, Gohlsch B, Hamalainen N, Staron RS, Uber A, Wehrle U, Pette D, 1993. Fast myosin heavy chain diversity in skeletal muscles of the rabbit: heavy chain IId, not IIb predominates. Eur. J. Biochem 211, 367–372. [PubMed: 8425546]

Alexander JJ, Quigg RJ, 2007. The simple design of complement factor H: looks can be deceiving. Mol. Immunol 44, 123–132. [PubMed: 16919753]

Alexander JJ, Jacob A, Bao L, Macdonald RL, Quigg RJ, 2005. Complement-dependent apoptosis and inflammatory gene changes in murine lupus cerebritis. J. Immunol 175, 8312–8319. [PubMed: 16339572]

Alexander JJ, Sankaran JS, Seldeen KL, Thiyagarajan R, Jacob A, Quigg RJ, Troen BR, Judex S, 2018. Absence of complement factor H alters bone architecture and dynamics. Immunobiology 223 (12), 761–771. [PubMed: 30107932]

Araujo KP, Bonuccelli G, Duarte CN, Gaiad TP, Moreira DF, Feder D, Belizario JE, Miglino MA, Lisanti MP, Ambrosio CE, 2013. Bortezomib (PS-341) treatment decreases inflammation and partially rescues the expression of the dystrophin-glycoprotein complex in GRMD dogs. PLoS One 8, e61367. [PubMed: 23579193]

Ashizawa T, Appel SH, 1985. Complement-dependent lysis of cultured rat myotubes by myasthenic immunoglobulins. Neurology 35, 1748–1753. [PubMed: 4069366]

Behan WM, Behan PO, 1977. Complement abnormalities in polymyositis. J. Neurol. Sci 34, 241–246. [PubMed: 925712]

Bloemberg D, Quadrilatero J, 2012. Rapid determination of myosin heavy chain expression in rat, mouse, and human skeletal muscle using multicolor immunofluorescence analysis. PLoS One 7, e35273. [PubMed: 22530000]

Bonington A, Whitmore I, Mahon M, 1987. A histological and histochemical study of the cricopharyngeus muscle in the guinea-pig. J. Anat 153, 151–161. [PubMed: 2962971]

Booth FW, Chakravarthy MV, Spangenburg EE, 2002. Exercise and gene expression: physiological regulation of the human genome through physical activity. J. Physiol 543, 399–411. [PubMed: 12205177]

Bottinelli R, Schiaffino S, Reggiani C, 1991. Force-velocity relations and myosin heavy chain isoform compositions of skinned fibres from rat skeletal muscle. J. Physiol 437, 655–672. [PubMed: 1890654]

Bredman JJ, Weijs WA, Moorman AF, 1992. Presence of cardiac alpha-myosin correlates with histochemical myosin Ca2+ ATPase activity in rabbit masseter muscle. Histochem. J 24, 260–265. [PubMed: 1535066]

Buckingham M, Alonso S, Barton P, Cohen A, Daubas P, Garner I, Robert B, Weydert A, 1986. Actin and myosin multigene families: their expression during the formation and maturation of striated muscle. Am. J. Med. Genet 25, 623–634. [PubMed: 3789022]

Cayci T, Kurt YG, Akgul EO, Kurt B, 2012. Does mtDNA copy number mean mitochondrial abundance? J. Assist. Reprod. Genet 29, 855. [PubMed: 22644635]

Ceddia RB, William WN Jr., Lima FB, Flandin P, Curi R, Giacobino JP, 2000. Leptin stimulates uncoupling protein-2 mRNA expression and Krebs cycle activity and inhibits lipid synthesis in isolated rat white adipocytes. Eur. J. Biochem 267, 5952–5958. [PubMed: 10998055]

Charrier EE, Janmey PA, 2016. Mechanical properties of intermediate filament proteins. Methods Enzymol 568, 35–57. [PubMed: 26795466]

Clarke M, Schatten G, Mazia D, Spudich JA, 1975. Visualization of actin fibers associated with the cell membrane in amoebae of Dictyostelium discoideum. Proc. Natl. Acad. Sci. U. S. A 72, 1758–1762. [PubMed: 1057168]

Cornelio F, Dones I, 1984. Muscle fiber degeneration and necrosis in muscular dystrophy and other muscle diseases: cytochemical and immunocytochemical data. Ann. Neurol 16, 694–701. [PubMed: 6524876]

Eckes B, Dogic D, Colucci-Guyon E, Wang N, Maniotis A, Ingber D, Merckling A, Langa F, Aumailley M, Delouvee A, et al. , 1998. Impaired mechanical stability, migration and contractile capacity in vimentin-deficient fibroblasts. J. Cell. Sci 111 (Pt 13), 1897–1907. [PubMed: 9625752]

Ferreira VP, Pangburn MK, Cortes C, 2010. Complement control protein factor H: the good, the bad, and the inadequate. Mol. Immunol 47, 2187–2197. [PubMed: 20580090]

Galler S, 1994. Stretch activation of skeletal muscle fibre types. Pflugers Arch. 427, 384–386. [PubMed: 8072861]

Gulick J, Hewett TE, Klevitsky R, Buck SH, Moss RL, Robbins J, 1997. Transgenic remodeling of the regulatory myosin light chains in the mammalian heart. Circ. Res 80, 655–664. [PubMed: 9130446]

Guo M, Ehrlicher AJ, Mahammad S, Fabich H, Jensen MH, Moore JR, Fredberg JJ, Goldman RD, Weitz DA, 2013. The role of vimentin intermediate filaments in cortical and cytoplasmic mechanics. Biophys. J 105, 1562–1568. [PubMed: 24094397]

Hamalainen N, Pette D, 1993. The histochemical profiles of fast fiber types IIB, IID, and IIA in skeletal muscles of mouse, rat, and rabbit. J. Histochem. Cytochem 41, 733–743. [PubMed: 8468455]

Hinz B, 2015. The extracellular matrix and transforming growth factor-beta1: tale of a strained relationship. Matrix Biol. 47, 54–65. [PubMed: 25960420]

Hopken UE, Lu B, Gerard NP, Gerard C, 1997. Impaired inflammatory responses in the reverse arthus reaction through genetic deletion of the C5a receptor. J. Exp. Med 186, 749–756. [PubMed: 9271590]

Jiu Y, Peranen J, Schaible N, Cheng F, Eriksson JE, Krishnan R, Lappalainen P, 2017. Vimentin intermediate filaments control actin stress fiber assembly through GEF-H1 and RhoA. J. Cell. Sci 130, 892–902. [PubMed: 28096473]

Kouser L, Abdul-Aziz M, Nayak A, Stover CM, Sim RB, Kishore U, 2013. Properdin and factor h: opposing players on the alternative complement pathway “see-saw”. Front. Immunol 4, 93. [PubMed: 23630525]

Krick S, Shi S, Ju W, Faul C, Tsai SY, Mundel P, Bottinger EP, 2008. Mpv17l protects against mitochondrial oxidative stress and apoptosis by activation of Omi/HtrA2 protease. Proc. Natl. Acad. Sci. U. S. A 105, 14106–14111. [PubMed: 18772386]

Legoedec J, Gasque P, Jeanne JF, Fontaine M, 1995. Expression of the complement alternative pathway by human myoblasts in vitro: biosynthesis of C3, factor B, factor H and factor I. Eur. J. Immunol 25, 3460–3466. [PubMed: 8566038]

Mathey D, Schofer J, Schafer HJ, Hamdoch T, Joachim HC, Ritgen A, Hugo F, Bhakdi S, 1994. Early accumulation of the terminal complement-complex in the ischaemic myocardium after reperfusion. Eur. Heart J 15, 418–423. [PubMed: 8013522]

Moncman CL, Rindt H, Robbins J, Winkelmann DA, 1993. Segregated assembly of muscle myosin expressed in nonmuscle cells. Mol. Biol. Cell 4, 1051–1067. [PubMed: 8298191]

Morgan BP, Campbell AK, Compston DA, 1984. Terminal component of complement (C9) in cerebrospinal fluid of patients with multiple sclerosis. Lancet 2, 251–254. [PubMed: 6146808]

Nair KS, 2005. Aging muscle. Am. J. Clin. Nutr 81, 953–963. [PubMed: 15883415]

Naito AT, Sumida T, Nomura S, Liu ML, Higo T, Nakagawa A, Okada K, Sakai T, Hashimoto A, Hara Y, et al. , 2012. Complement C1q activates canonical Wnt signaling and promotes aging-related phenotypes. Cell 149, 1298–1313. [PubMed: 22682250]

Pacher P, Sharma K, Csordas G, Zhu Y, Hajnoczky G, 2008. Uncoupling of ER-mitochondrial calcium communication by transforming growth factor-beta. Am. J. Physiol. Renal Physiol 295, F1303–1312. [PubMed: 18653477]

Pangburn MK, 1988. Alternative pathway of complement. Methods Enzymol 162, 639–653. [PubMed: 2976114]

Pickering MC, Cook HT, Warren J, Bygrave AE, Moss J, Walport MJ, Botto M, 2002. Uncontrolled C3 activation causes membranoproliferative glomerulonephritis in mice deficient in complement factor H. Nat. Genet 31, 424–428. [PubMed: 12091909]

Powers SK, Lawler J, Criswell D, Lieu FK, Dodd S, 1992. Alterations in diaphragmatic oxidative and antioxidant enzymes in the senescent Fischer 344 rat. J. Appl. Physiol 72 (1985), 2317–2321. [PubMed: 1629087]

Puri TS, Quigg RJ, 2007. The many effects of complement C3- and C5-binding proteins in renal injury. Semin. Nephrol 27, 321–337. [PubMed: 17533009]

Rangaraju V, Calloway N, Ryan TA, 2014. Activity-driven local ATP synthesis is required for synaptic function. Cell 156, 825–835. [PubMed: 24529383]

Richmonds CR, Kaminski HJ, 2001. Nitric oxide synthase expression and effects of nitric oxide modulation on contractility of rat extraocular muscle. FASEB J. 15, 1764–1770. [PubMed: 11481224]

Saraste M, 1999. Oxidative phosphorylation at the fin de siecle. Science 283, 1488–1493. [PubMed: 10066163]

Sawada Y, Tamada M, Dubin-Thaler BJ, Cherniavskaya O, Sakai R, Tanaka S, Sheetz MP, 2006. Force sensing by mechanical extension of the Src family kinase substrate p130Cas. Cell 127, 1015–1026. [PubMed: 17129785]

Schafer H, Mathey D, Hugo F, Bhakdi S, 1986. Deposition of the terminal C5b-9 complement complex in infarcted areas of human myocardium. J. Immunol 137, 1945–1949. [PubMed: 3528291]

Schiaffino S, Reggiani C, 2011. Fiber types in mammalian skeletal muscles. Physiol. Rev 91, 1447–1531. [PubMed: 22013216]

Schiaffino S, Gorza L, Sartore S, Saggin L, Ausoni S, Vianello M, Gundersen K, Lomo T, 1989. Three myosin heavy chain isoforms in type 2 skeletal muscle fibres. J. Muscle Res. Cell. Motil 10, 197–205. [PubMed: 2547831]

Seldeen KL, Lasky G, Leiker MM, Pang M, Personius KE, Troen BR, 2017. High Intensity Interval Training (HIIT) improves physical performance and frailty in aged mice. J. Gerontol. A Biol. Sci. Med. Sci 73 (4), 429–437.

Sewry CA, Dubowitz V, Abraha A, Luzio JP, Campbell AK, 1987. Immunocytochemical localisation of complement components C8 and C9 in human diseased muscle. The role of complement in muscle fibre damage. J. Neurol. Sci 81, 141–153. [PubMed: 3694223]

Shortreed KE, Krause MP, Huang JH, Dhanani D, Moradi J, Ceddia RB, Hawke TJ, 2009. Muscle-specific adaptations, impaired oxidative capacity and maintenance of contractile function characterize diet-induced obese mouse skeletal muscle. PLoS One 4, e7293. [PubMed: 19806198]

Sorgenfrei J, Damerau B, Vogt W, 1982. Role of histamine in the spasmogenic effect of the complement peptides C3a and C5a-desArg (classical anaphylatoxin). Agents Actions 12, 118–121. [PubMed: 6177210]

Spuler S, Engel AG, 1998. Unexpected sarcolemmal complement membrane attack complex deposits on nonnecrotic muscle fibers in muscular dystrophies. Neurology 50, 41–46. [PubMed: 9443455]

Staron RS, Malicky ES, Leonardi MJ, Falkel JE, Hagerman FC, Dudley GA, 1990. Muscle hypertrophy and fast fiber type conversions in heavy resistance-trained women. Eur. J. Appl. Physiol. Occup. Physiol 60, 71–79. [PubMed: 2311599]

Tang DD, Gerlach BD, 2017. The roles and regulation of the actin cytoskeleton, intermediate filaments and microtubules in smooth muscle cell migration. Respir. Res 18, 54. [PubMed: 28390425]

Traub P, Shoeman RL, 1994. Intermediate filament proteins: cytoskeletal elements with gene-regulatory function? Int. Rev. Cytol 154, 1–103. [PubMed: 8083030]

Walport MJ, 2001a. Complement. First of two parts. N. Engl. J. Med 344, 1058–1066. [PubMed: 11287977]

Walport MJ, 2001b. Complement. Second of two parts. N. Engl. J. Med 344, 1140–1144. [PubMed: 11297706]

Wang HA, Lee JD, Lee KM, Woodruff TM, Noakes PG, 2017. Complement C5a-C5aR1 signalling drives skeletal muscle macrophage recruitment in the hSOD1 (G93A) mouse model of amyotrophic lateral sclerosis. Skelet. Muscle 7, 10. [PubMed: 28571586]

Yoon YS, Lee JH, Hwang SC, Choi KS, Yoon G, 2005. TGF beta1 induces prolonged mitochondrial ROS generation through decreased complex IV activity with senescent arrest in Mv1Lu cells. Oncogene 24, 1895–1903. [PubMed: 15688038]

Zhang C, Wang C, Li Y, Miwa T, Liu C, Cui W, Song WC, Du J, 2017. Complement C3a signaling facilitates skeletal muscle regeneration by regulating monocyte function and trafficking. Nat. Commun 8, 2078. [PubMed: 29233958]

Zipfel PF, Skerka C, 2009. Complement regulators and inhibitory proteins. Nat. Rev. Immunol 9, 729–740. [PubMed: 19730437]

Zong H, Ren JM, Young LH, Pypaert M, Mu J, Birnbaum MJ, Shulman GI, 2002. AMP kinase is required for mitochondrial biogenesis in skeletal muscle in response to chronic energy deprivation. Proc. Natl. Acad. Sci. U. S. A 99, 15983–15987. [PubMed: 12444247]

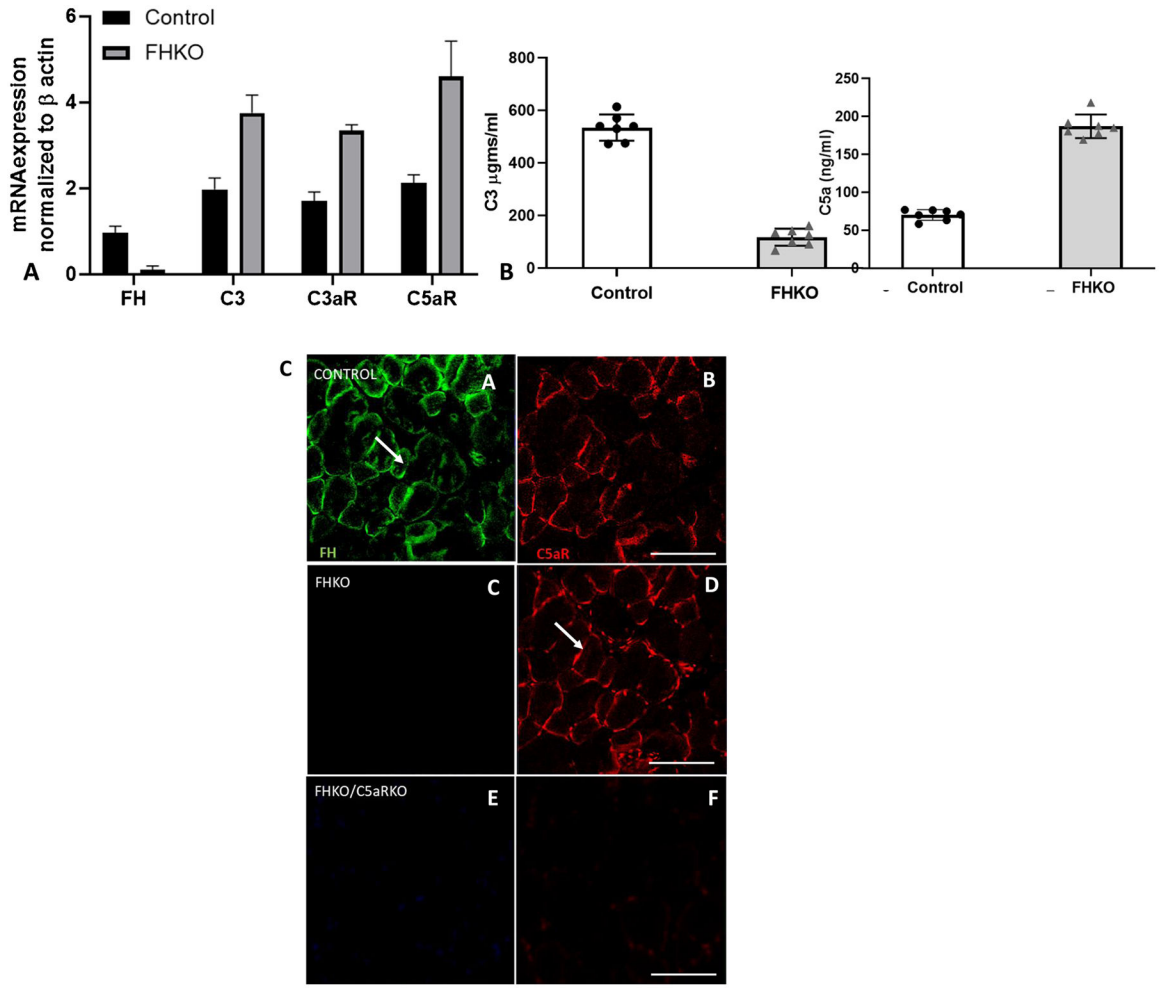

Fig. 1.

A. mRNA expression of muscle C3, C3aR and C5aR are increased in the absence of FH. Gene expression levels of complement proteins FH, C3, C3aR and C5aR were determined in gastrocnemius muscles (GCN) of fh−/− and wt mice. Real-time quantitative RT-PCR analyses of the mRNA levels were performed on total RNA samples from the GCN of the mice. Primer sequences used are shown in Table 1. Data are expressed as Means ± SD (n = 8). fh−/− mice vs. WT mice: *$P < 0.05$; **$P < 0.01$.

B. C3 is decreased and C5a is increased in plasma of fh−/− mice.

C3 and C5a were measured in the plasma of fh−/− (●) and WT (●) mice (n = 8/group) by ELISA as described in the Methods. C3 is decreased while C5a is increased significantly in circulation in fh−/− mice compared to controls, $p < 0.05$.

C. FH and C5aR are expressed in the rodent GCN muscle.

Given are representative immunofluorescence images of FH and C5aR expression in GCN muscle. 10 um cryo sections were stained using anti-FH (1:250) and anti-C5aR (1:100) overnight and detected with Alex 488 –anti-goat and Alex 564 anti-rabbit. Green, FH and red, C5aR. FH and C5aR stain the muscle membranes as indicated by the arrow.

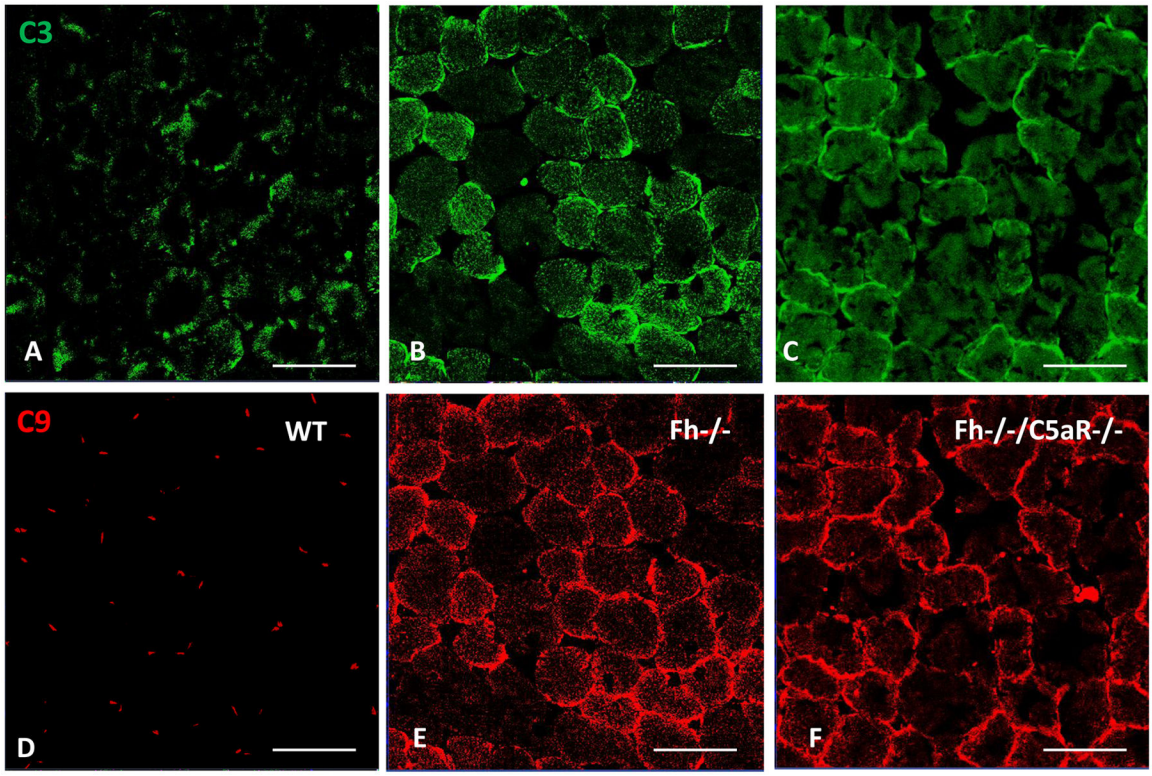

Fig. 2.

FH deletion increases C3 and C9 deposits in muscle.

Representative muscle cryosections ($n = 8$) from 16 wk fh−/− and control mice reveal significant increase in C3d (green) and C9 (red) deposits in muscle which remained unchanged in fh−/−/C5aR−/− double knockouts. A and D are from control mice, B and E from fh−/− mice and C and F from fh−/−C5aR−/− mice respectively. A, B and C are sections stained for FITC labeled C3; D, E and F are sections stained for Alexa 594 labeled C9. Bar represents 100 μm.

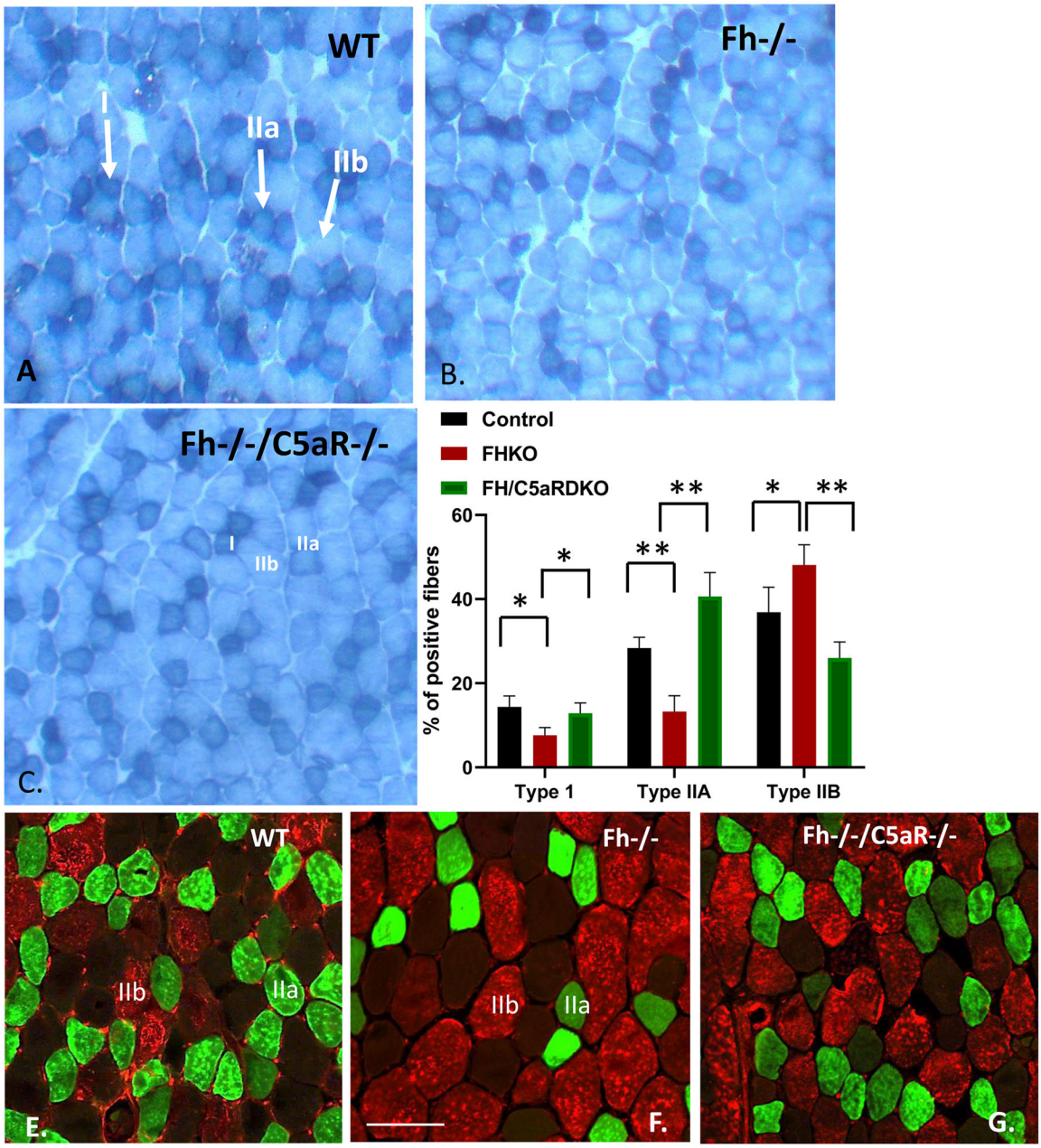

Fig. 3.

C5aR inhibition protects muscle fiber changes in FH deficient muscle.

To determine the impact of FH deficiency on muscle biology, gastrocnemius muscle (GCN) sections from 16 week fh−/− (B) and wild type (wt, A) male mice (n = 8) were stained for NADH (upper panel) The NADH stain of skeletal muscle show a mix of Type 1 (dark), Type IIB (light) and type IIA (medium color) muscle fibers. Type IIA fibers were reduced and IIB fibers were increased in FH deficient mice. The change was reduced in C5aR−/−/fH −/− DKO (C). The different fiber types were counted in whole sections from each mouse and calculated as the % of total fibers in the section. The Bar graph (D) gives the % of each fiber type in the section in WT, fh−/− and fh−/−/C5aR−/−DKO mice. *, $p < 0.05$, **, $p < 0.01$.

Given are representative gastrocnemius muscle sections ($n = 8$) from 16wk fh−/− (F), control (E) and fh−/−/ C5aR−/− mice. To assess muscle fiber-type profile, cryosections from all mice were incubated with cocktail of primary antibodies MHCIIA (SC-71, green), and MHCIIB (BF-F3, red), followed by incubation with appropriate fluorescent-conjugated secondary antibodies as described in Methods. Staining reveals reduction in Type IIA fibers (green) and increase in Type IIB fibers (red) in the absence of FH. The change in muscle fiber was reduced when C5aR was deleted in FH deficient (G) mice. The sections were observed using a 20X objective. The unstained regions represent both fiber type 1 and fiber type IIX. Bar represents 100 μm.

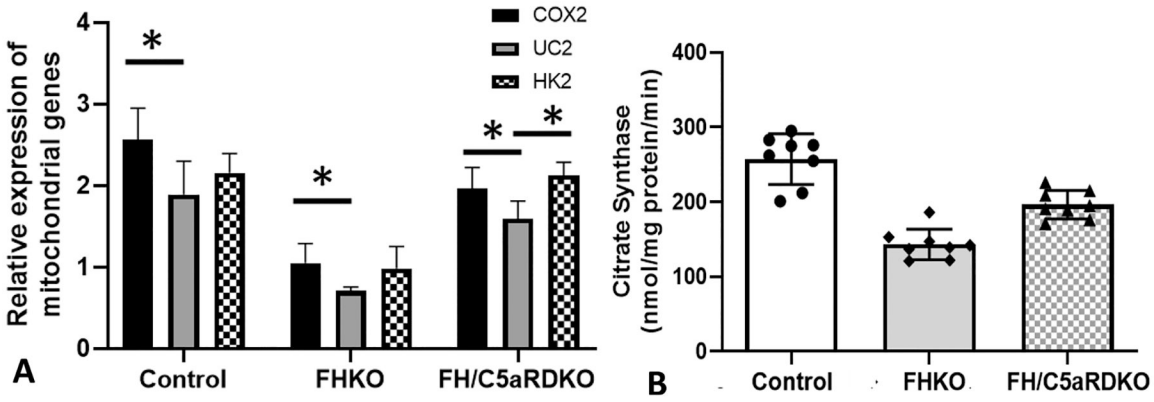

Fig. 4.

mtDNA content (A) and citrate synthase (CS) activity (B) are reduced in GCN muscles of fh−/− mice compared to control mice.

mtDNA expression of *Cox2, Ucp2* and *Hk2* were assessed in muscle from wt, fh−/− and fh−/−/C5aR DKO mice by qRT-PCR (A). Expression of *Cox2, Ucp2* and *Hk2* mtDNA were significantly reduced in fh−/− mice. Absence of C5a/C5aR signaling did not alter the trajectory of *Cox2* and *Ucp2* but prevented the decrease in *Hk2*. Citrate synthase (CS) activity was measured in muscle lysates from wt, fh−/− and fh−/−/C5aR DKO mice (B). The activity is normalized to the total protein content of the sample used in the assay. Normalized data are presented as Means ± SD. *P < 0.05.

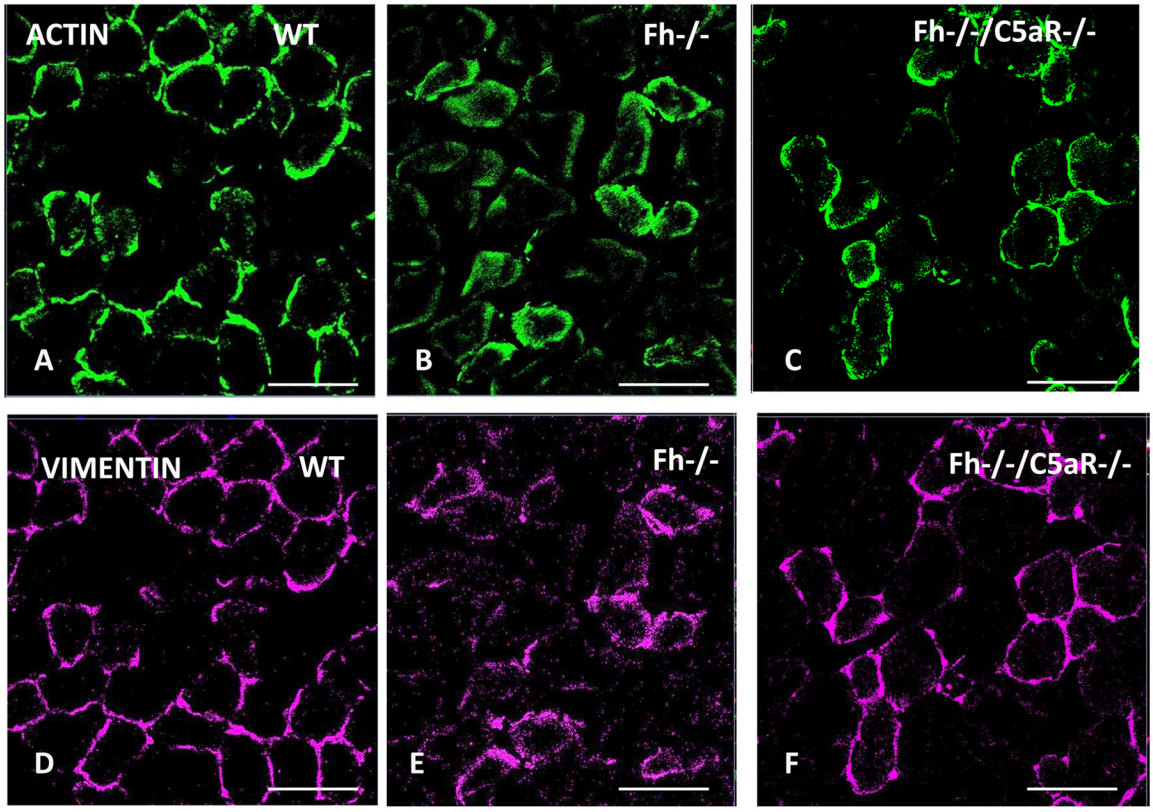

Fig. 5.

FH deletion increases expression of cytoskeletal proteins in muscle in C57BL6 mice. Expression levels of cytoskeletal proteins actin and vimentin were determined in gastrocnemius muscles (GCN) of fh−/− and wt mice. Cryosections of the muscle were stained with actin (green) and vimentin (pink). Representative images are given. Actin and vimentin displayed defined pattern along the cell perphery (Fig. 5A & D) which changed to less defined localization within the cell (Fig. 5B & E). The vimentin and actin localization was more defined along the periphery in the absence of C5a/C5aR signaling (Fig. 5C & F). Bar: 100 μm.

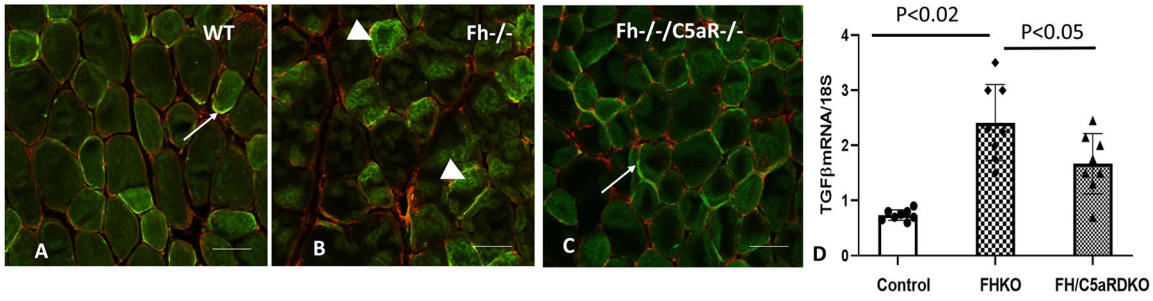

Fig. 6.

FH deletion increases expression of TGFβ in muscle in C57BL6 Mice.

Expression level of TGFβ was determined in gastrocnemius muscles (GCN) of fh−/− and fh−/−C5aR−/− mice at both the transcriptional and translational levels. Cryosections of the muscle were stained with anti-TGFβ. Representative images are given. TGFβ occurs in the sarcoplasmic membrane in the controls. In the absence of FH, TGFβ expression is seen in the endomysium (Fig. 6B) compared to controls (Fig. 6A) which was reduced in the absence of C5a/C5aR signaling (Fig. 6C). 40X; bar: 50 μm. In line with this observation, TGFβ RNA expression was increased in the FHKO by real-time PCR (Fig. 6D). Data are expressed as means ± SE (n = 8 per group).

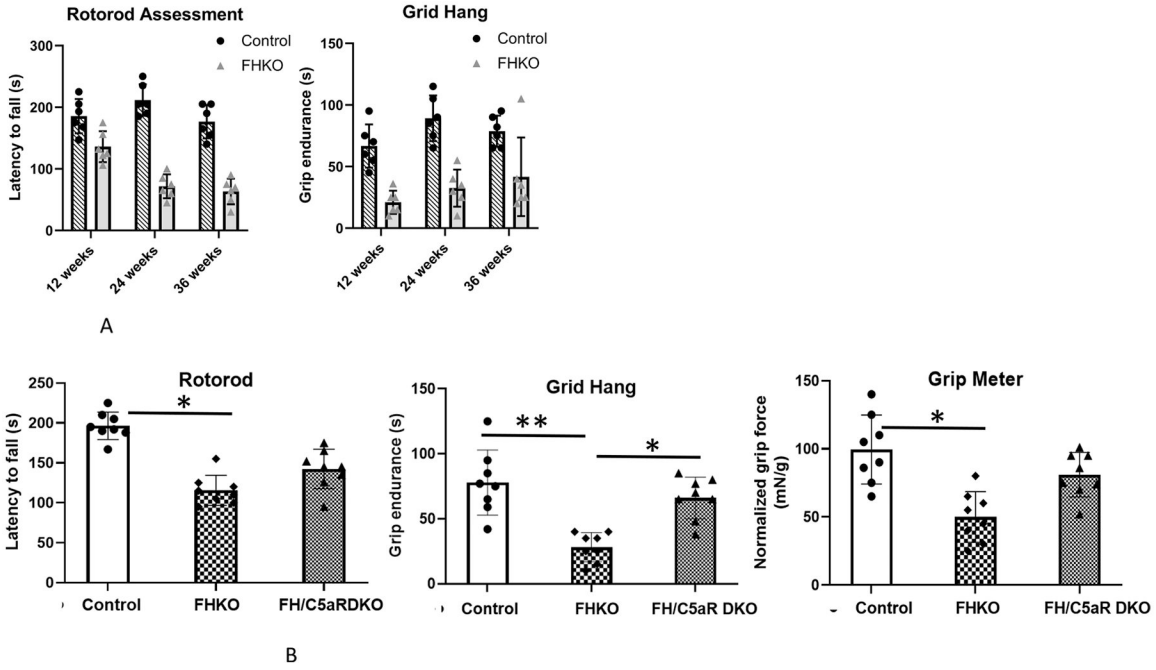

Fig. 7.

A. Absence of FH alters muscle performance.

Muscle performance and strength were assessed at 12 weeks (preclinical) and at 24 weeks (disease). Results show that the change in rotorod (A) and grid hang (B) occurred at 12 weeks and continued albeit with considerable variability at 24 weeks. Values are expressed as Mean ± SD. *$p < 0.05$, **$p < 0.01$.

B. Absence of C5a/C5aR signaling prevents reduced physical performance in fh−/− muscle. Given are assessments for muscle performance (motor function, strength and coordination) in 16 week $fh^{-/-}$, fh−/−C5aR−/− and wildtype (wt) mice ($n = 8$). Reduced performance is observed in the three assessments (rotarod, grip meter and grid hang) and there was no change in treadmill assessment (results not shown) in fh−/− mice while C5aR deficiency prevented the changes. Values are expressed as Mean ± SD. *$P < 0.05$.

Table 1

List of antibodies used for MHC staining of mouse skeletal muscle.

Species	Primary Antibody		Secondary Antibody
Mouse	SC-71 (1:600)	IIA	Alexa Fluor 488 IgG1 1:500 (green)
	BF-F3 (1:100)	IIB	Alexa Fluor 555 IgM 1:500 (red)
	C3 (1:250)		FITC coupled antibody
	TgFβ (1:100)		Alexa Fluor 488 IgG1 1:500 (green)

Table 2

Primer sequences.

Gene	Forward primer	Reverse primer
Complement proteins		
C3	ATGCTGACCCTGAGGTCAAA	GGCCTTCTCTCTAACAGCCA
C3aR	ATTGGGACTGCTAGGCAATG	GGTGAGATGGAGGAACCAGA
C5aR	TTACCACAGAACCCAGGAGG	GCCATCCGCAGGTATGTTAG
FH	TCTCAGGCTCGTGGTCAGAA	CCAGGGCGGCATTTGTAG
mt DNA		
Cox2	GTTGATAACCGAGTCGTTCTGC	CCTGGGATGGCATCAGTTTT
Ucp2	CTACAGATGTGGTAAAGGTCCGC	GCAATGGTCTTGTAGGCTTCG
Hk2	TCTGGCTCTGAGATCCATCTTCA	CCGGCCTCTTAACCACATTCC
nuclear DNA		
B-Globulin	CTT CTG GCT ATG TTT CCC TT	GTT CTC AGG ATC CAC ATG CA
18s	CCGCAAGGGAAAGATGAAAGAC	TCGTTTGGTTTCGGGGTTTC
TGFβ	ATACGCCTGAGTGGCTGTCT	TGGGACTGATCCCATTGATT

Immunobiology. Author manuscript; available in PMC 2023 January 17.

Table 3

Effect of FH on weight, fat and circulating calcium.

	WT	fh−/−	P value	n
Weight (g)	29±2	32±3.4	0.065	8
Fat%	21±4	28±5	0.06	8
Calcium (nmol/L)	9.8±0.19	9.6 + 0.15	0.22	8